THE AMERICAN SOCIETY OF MECHANICAL ENGINEERS
345 E. 47th St., New York, N.Y. 10017

95-GT-265

NUMERICAL ANALYSIS OF FLUID FLOW IN AN INTERNAL TURBINE BLADE COOLING PASSAGE

Using a Second Order TVD Scheme with κ-ω Turbulence Model

Marc L Babich, Song-Lin Yang, Donna J Michalek, and Oner Arici

Mechanical Engineering - Engineering Mechanics Department
Michigan Technological University
Houghton, Michigan

ABSTRACT

The need to develop ultra-high efficiency turbines demands the exploration of methods which will improve the thermal efficiency and the specific thrust of the engine. One means of achieving these goals is to increase the turbine inlet temperature. In order to accomplish this, further advances in turbine blade cooling technology will have to be realized. A technique which has only recently been used in the analysis of turbine blade cooling is computational fluid dynamics. The purpose of this paper is to present a numerical study of the flowfield inside of the internal cooling passage of a radial turbine blade. The passage is modeled as two-dimensional and non-rotating. The flowfield solutions are obtained using a pseudo-compressible formulation of the Navier-Stokes equations. The spatial discretization is performed using a symmetric second-order accurate TVD (Total Variational Diminishing) scheme. Calculations are performed on a multi-block-structured grid. Turbulence is modeled using a modified κ-ω model. In the absence of experimental data, results appear to be realistic based on common experiences with fluid mechanics.

NOMENCLATURE

Variables

C	reference length
C_ω	cross-diffusion term
D	destruction terms
F	convective flux vector in x direction
F_v	diffusive flux vector in x direction
G	convective flux vector in y direction
G_v	diffusive flux vector in y direction
P	production terms
p	static pressure = $\left(p^* - p_{amb}\right)/\left(\rho u_\infty\right)$
Re	Reynolds number = $\rho u_\infty C/\mu$
S	Source term containing production, destruction, and cross-diffusion terms
t	time
U	vector containing dependent variables
u	x component velocity
v	y component velocity
x	x-coordinate
y	y-coordinate
β	pseudo-compressibility factor
ρ	density
κ	turbulent kinetic energy
μ	viscosity
ω	specific dissipation rate

Subscripts

amb	ambient
t	turbulent
∞	inlet values

INTRODUCTION

The need to develop ultra-high efficiency gas turbines requires the exploration of methods which will improve the thermal efficiency and thrust of the engine. One means of accomplishing these goals is to increase the turbine inlet temperature. Due to the temperature limits imposed by the blade materials, the implementation of higher inlet temperatures requires investigation into new materials and/or improved cooling techniques, the latter option being the focus of this work. While the idea of using forced internal convection to cool the blades was first proposed several decades ago (Cohen et al., 1987), it is only recently that computational fluid dynamics (CFD) codes have been used in this effort. CFD codes

Presented at the International Gas Turbine and Aeroengine Congress and Exposition
Houston, Texas - June 5-8, 1995

can be used to further enhance understanding of heat transfer and fluid flow in turbine blades, and it can also help reduce the expensive cost of experimentation by reducing the number of needed experiments.

Attempts have been made to study the cooling passages using parabolic marching techniques (Katsanis, 1985, and Majumdar et al., 1977) for simple rectangular flow passages. These attempts achieved only limited success for the simple geometries to which they were applied. The more realistic geometry of the radial turbine blade shown in Figure 1 presents a far greater challenge. A numerical study was conducted on this geometry using a one-dimensional code by Kumar et al. (1989). While this code was able to account for the geometry of the actual turbine blade, no one-dimensional code will ever be able to give the detailed information needed in the design and development stages. Use of this type of code in the design stage will not significantly reduce the amount of testing needed in the development of an optimum cooling passage geometry. It is felt that in order to truly be useful in the design stage, a computer model must be both robust and multi-dimensional. In order to develop a fundamental understanding of the physics behind duct flow under rotation, Tekriwal (1994) and Prakash and Zerkle (1992) performed studies using κ-ε turbulence models on simple rectangular ducts undergoing rotation similar to what a turbine blade experiences. A three-dimensional, rotating study of this particular geometry was performed by Dawes (1994) using an adaptive, unstructured grid with a κ-ε turbulence model. Stephens et al. (1993) also modeled this geometry without rotation using a Chimera grid system. The biggest uncertainty in these studies is the performance of the turbulence model. Recent studies have shown that the κ-ω model may be better at predicting turbulent flows (Wilcox, 1993b). This paper presents a study of a two-dimensional turbine blade cooling passage with no rotation as a preliminary study in our attempt to develop a rotating, three-dimensional CFD code with a κ-ω turbulence model for use in design optimization.

The code that is being used for this study is a pseudo-compressible code that uses a spatially second-order accurate TVD (Total Variational Diminishing) scheme developed at Michigan Technological University (MTU). This code has previously given excellent results for other geometries, in particular, wind turbine airfoils (Yang et al.,1994b). The original version of the code was developed for single-block meshes. Because of the complicated geometry of the internal cooling passages (Figure 1), it was decided to utilize a block-structured grid. One of the advantages of using a block-structured grid is that any complicated geometry can be broken up into several basic geometrical segments. Also, during the design process, changes are sometimes made only in certain regions. Because of this, using a block-structured grid is an advantage in that only the areas affected by the geometry changes need to be re-generated.

Because of the geometrical complexity of the turbine blade cooling passage, especially the pin fins, turbulence will play an important role in the dynamics of the flow. Therefore, an advanced turbulence model must be used. Numerical studies of turbulent incompressible flows based on the Navier-Stokes (N-S) equations can be classified into three major groups: (1) direct simulation, (2) large-eddy simulation, and (3) time-averaged N-S

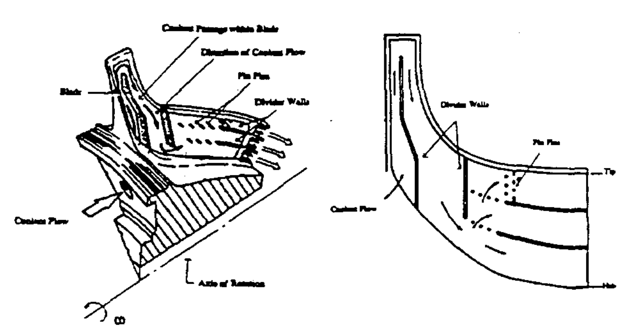

FIGURE 1: SCHEMATIC OF TURBINE BLADE WITH A COOLING PASSAGE INSIDE OF IT

equations (Reynolds, 1976; Bradbury, et al., 1982; Haines, 1982; Lakshminarayana, 1986). For turbulent flows of engineering interest, current computing capabilities only permit numerical analysis of the time-averaged N-S equations closed by a turbulent model. Among all the available and practical turbulence models currently in use in the CFD research community, the two most popular and versatile turbulent models are the κ-ε (specific turbulence kinetic energy-turbulence kinetic energy dissipation) models (Launder and Spalding, 1974) and the κ-ω (specific turbulence kinetic energy dissipation rate) models (Menter, 1994; Wilcox, 1993a). Both of these two models have shown some successful results in simulating either wall-bounded and/or free-shear flows.

Using a combination of singular perturbation methods and numerical computations, Wilcox demonstrated that conventional κ-ε models generally are very inaccurate for boundary layers with adverse pressure gradient, even when the gradient is mild. He found that a more suitable choice of dependent variables, namely κ-ω, exists that is much more accurate for adverse pressure gradients (Wilcox, 1993a, 1993b, 1994). This has been shown to be true for airflow over a wind turbine airfoil (Yang, 1995a).

In this study, the cooling passage shown in Figure 1 will be modeled. The steady flow is modeled as turbulent, viscous, and incompressible. In addition, rotation is not included so that future comparisons can be made with experiments performed under stationary conditions. Preliminary numerical results of velocity and pressure are given.

MATHEMATICAL FORMULATION

The time-averaged N-S equations are formulated using the pseudo-compressible formulation (Chorin, 1967; Kwak et al., 1986; Yang et al. 1994a, 1994b). These equations (normalized), written in compact conservative vector form in Cartesian coordinates, are:

$$\frac{\partial U}{\partial t} + \frac{\partial F}{\partial x} + \frac{\partial G}{\partial y} = \frac{\partial F_v}{\partial x} + \frac{\partial G_v}{\partial y} \qquad (1)$$

where

$$U = \begin{bmatrix} p \\ u \\ v \end{bmatrix} \quad F = \begin{bmatrix} \beta u \\ u^2 + p \\ uv \end{bmatrix} \quad G = \begin{bmatrix} \beta v \\ uv \\ v^2 + p \end{bmatrix} \tag{2}$$

$$F_v = \begin{bmatrix} 0 \\ \frac{2\left(1 + \mu_t/\mu\right)}{Re}\frac{\partial u}{\partial x} - \frac{2}{3}\kappa \\ \frac{1 + \mu_t/\mu}{Re}\left(\frac{\partial u}{\partial y} + \frac{\partial v}{\partial x}\right) \end{bmatrix} \quad G_v = \begin{bmatrix} 0 \\ \frac{1 + \mu_t/\mu}{Re}\left(\frac{\partial u}{\partial y} + \frac{\partial v}{\partial x}\right) \\ \frac{2\left(1 + \mu_t/\mu\right)}{Re}\frac{\partial v}{\partial y} - \frac{2}{3}\kappa \end{bmatrix} \tag{3}$$

The vector U in equation (2) contains the normalized dependent variables: pressure, x- and y-component velocities. Vectors F and G are the x and y convection fluxes, respectively, and F_v and G_v correspond to the diffusion fluxes in the respective x and y directions. The parameter β in the column vectors F and G is the pseudo-compressibility factor and is set equal to 1.0, based on the parametric study of Yang et al. (1995b). The κ, μ, and μ_t in vectors F_v and G_v are the specific turbulence kinetic energy, the molecular viscosity, and the eddy viscosity, respectively, and will be described in greater detail later.

The variables are non-dimensionalized using a characteristic scale, C, as well as the inlet velocity and ambient pressure. The Reynolds number, Re, is defined on the basis of the characteristic length, i.e., $Re = (\rho u_\infty C)/\mu$.

These equations are transformed to the computational domain where the calculations are performed. The specifics of this transformation and the resulting equations can found in Yang et al. (1994a,1994b) and will not be repeated here. The numerical method that is employed uses one of Yee's spatially second-order symmetric TVD schemes to approximate the convective fluxes (Yee et al., 1987, and Yee et al., 1990). The diffusion terms are centrally differenced. The resulting equations can be found in Yang et al. (1994a,1994b).

Turbulence Model

Wilcox's modified κ–ω turbulence model (1993a, 1993b, 1994) is used in all computations to determine μ_t, κ, and ω. The modified version of this model is based on the Wilcox's high-Reynolds number model (1988) with the following modifications: (1) account for the near wall low-Reynolds number effects so that the model equations can be integrated through the viscous sublayer (Wilcox 1992), and (2) include the cross-diffusion term in the ω equation to reduce the model's sensitivity to the freestream ω value (Wilcox 1993b). The non-dimensionalized κ–ω turbulence model equations, in compact conservative vector form in Cartesian coordinates, are:

$$\frac{\partial U_t}{\partial t} + \frac{\partial F_t}{\partial x} + \frac{\partial G_t}{\partial y} = \frac{\partial F_{vt}}{\partial x} + \frac{\partial G_{vt}}{\partial y} + S \tag{4}$$

where

$$U_t = \begin{bmatrix} \kappa \\ \omega \end{bmatrix} \quad F_t = \begin{bmatrix} u\kappa \\ u\omega \end{bmatrix} \quad G_t = \begin{bmatrix} v\kappa \\ v\omega \end{bmatrix} \tag{5}$$

$$F_{vt} = \frac{1}{Re}\begin{bmatrix} \left(1 + \sigma^*\frac{\mu_t}{\mu}\right)\frac{\partial \kappa}{\partial x} \\ \left(1 + \sigma\frac{\mu_t}{\mu}\right)\frac{\partial \omega}{\partial x} \end{bmatrix} \quad G_{vt} = \frac{1}{Re}\begin{bmatrix} \left(1 + \sigma^*\frac{\mu_t}{\mu}\right)\frac{\partial \kappa}{\partial y} \\ \left(1 + \sigma\frac{\mu_t}{\mu}\right)\frac{\partial \omega}{\partial y} \end{bmatrix} \tag{6}$$

$$S = \begin{bmatrix} P_\kappa + D_\kappa \\ P_\omega + D_\omega + C_\omega \end{bmatrix} \tag{7}$$

In the above equations, U_t is the vector of normalized dependent variables consisting of κ and ω. F_t and G_t are the convection fluxes in the x and y directions, respectively. Similarly, F_{vt} and G_{vt} are the diffusion fluxes in the respective x and y directions. The source term vector, S, contains the production (P_κ and P_ω), destruction (D_κ and D_ω), and cross-diffusion (C_ω) terms. These terms are expressed as:

$$\begin{aligned} P_\kappa &= \alpha^*\frac{\kappa}{\omega}\Omega^2 \\ D_\kappa &= -B^*\omega\kappa \\ P_\omega &= \alpha\alpha^*\Omega^2 \\ D_\omega &= -B\omega^2 \\ C_\omega &= max\left[0, \frac{\sigma_d}{\omega}\left(\frac{\partial\kappa\partial\omega}{\partial x\partial x} + \frac{\partial\kappa\partial\omega}{\partial y\partial y}\right)\right] \end{aligned} \tag{8}$$

where Ω in the production terms is expressed as

$$\Omega = \sqrt{\left(\frac{\partial u}{\partial y} + \frac{\partial v}{\partial x}\right)^2 + 2\left[\left(\frac{\partial u}{\partial x}\right)^2 + \left(\frac{\partial v}{\partial y}\right)^2\right]} \tag{9}$$

The modified modeling closure coefficients are

$$\begin{aligned} \alpha^* &= \frac{R_\kappa\alpha_0^* + Re_t}{R_\kappa + Re_t} \\ \alpha &= \frac{1}{2}\frac{R_\omega\alpha_0 + Re_t}{\left(R_\omega + Re_t\right)\alpha^*} \\ B^* &= \frac{9}{100}\frac{5/18 + \left(Re_t/R_\beta\right)^4}{1 + \left(Re_t/R_\beta\right)^4} \end{aligned} \tag{10}$$

and

$$B = \frac{3}{40} \quad \sigma^* = 1 \quad \sigma = \frac{3}{5} \quad \alpha_0^* = \frac{B}{3} \quad \alpha_0 = \frac{1}{10}$$

$$\sigma_d = \frac{3}{10} \quad R_\beta = 8 \quad R_\kappa = 6 \quad R_\omega = \frac{11}{5} \tag{11}$$

in which the turbulent Reynolds number (Re_t) is defined as

$$Re_t = Re\frac{k}{\omega} \tag{12}$$

and the ratio of the eddy viscosity to the molecular viscosity (μ_t/μ), in terms of Re_t, is expressed as:

$$\frac{\mu_t}{\mu} = \alpha^* Re_t \quad (13)$$

PHYSICAL PROBLEM

Grid Generation

In order to carry out the computations, the domain of interest must be reduced to a finite grid system. This can be done in any number of ways. The method used for this study was to employ an elliptic PDE grid generator. A Poisson-type equation was formulated based on the work done by Steger and Sorenson (1979) with the addition of extra source terms that would control orthogonality and grid spacing at an additional boundary. Due to the geometrical complexity of the cooling passage, the domain was divided into five separate blocks (Figure 2). The grid for each block was generated separately and then patched together to form the grid system for the entire cooling passage (Figure 3). This grid contains 7629 active vertices.

Block-Structured Grid

When a typical single-block mesh is used, calculations can be carried out on the grid points row by row implicitly. However, since the cooling passage was divided into several blocks of different sizes, a different method of cycling through the grid points was required. There are two principal ways to do this. The first method solves each block independently of the others and uses the information from connecting blocks as part of the boundary conditions. This method can pose several problems such as programming complexity, proliferate exchange of data when switching from one block to the next, and large memory requirements. The other method "eliminates" the block structure of the grid and performs calculations on one grid point at a time. The main drawback of this method is that it must use explicit computational techniques which can take longer than implicit ones. However, with the speed of computers today as well as parallel processing, explicit point-by-point methods are becoming popular once again.

Since calculations are carried out one grid point at a time, the labeling of each point using two indices, i.e. (i,j), is no longer necessary. Therefore, each grid point is referenced only with a single index, (i4), with additional arrays which specify the connectivity of the grid points. This is similar to the data structure used for an unstructured grid and also in KIVA-3 (Amsden, 1993). An example of this can be seen in Figure 4.

One additional benefit of using this approach, is that the grid points can be sorted in such a manner as to make calculations more efficient, as is done in KIVA-3. At the start of calculations, the grid points are sorted so that those with the lower index range are inactive vertices which are not used in the calculations (used mainly for easier pre- and post-processing). The next range of vertices are those which are interior grid points which are used most often. At the end are all of the boundary vertices that are only updated at the end of each iteration. By sorting the vertices in this manner, significant amounts of time can be saved since each vertex will not have to be tested at every iteration to determine whether it lies on a boundary, inside a solid surface, or in the fluid.

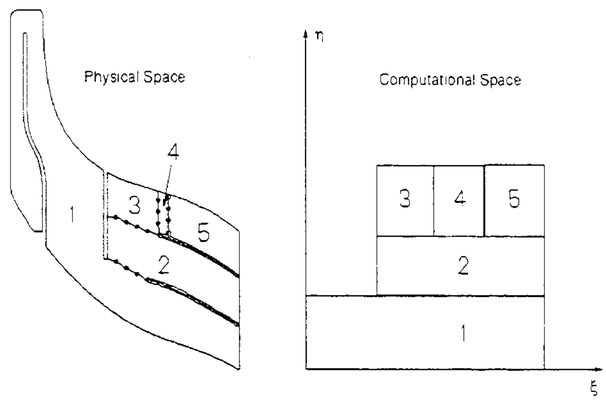

FIGURE 2: PHYSICAL AND COMPUTATIONAL SPACE

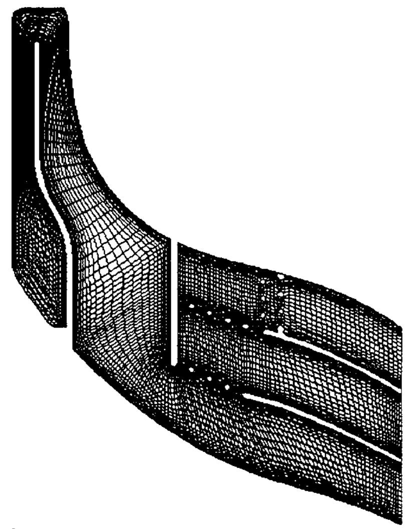

FIGURE 3: COOLING PASSAGE GRID

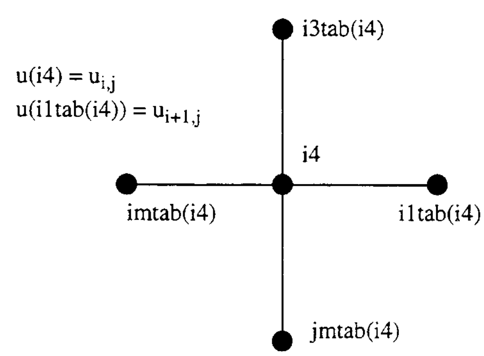

FIGURE 4: SINGLE INDEX AND CONNECTIVITY STRUCTURE

Boundary Conditions

Since viscous flow is being modeled, the no-slip boundary condition is applied at the solid surface, i.e., u=v=0 on the surface.

Accordingly, the turbulent kinetic energy is also equal to zero at the walls. Near the solid walls, ω must satisfy the following asymptotic solution (Wilcox, 1993a):

$$\omega \rightarrow \frac{2}{B^* Re\, y_n^2} \qquad \text{as } y_n \rightarrow 0 \qquad (14)$$

where y_n is the normal distance from the wall. To reduce the numerical errors for ω near a solid wall, this condition is enforced at the first grid point from the wall to achieve the proper limiting form. This procedure is also used by Liu and Zheng (1994) and Huang and Coakley (1992). The pressure on the solid wall is obtained by the zero normal pressure gradient approximation.

For comparison to experimental data, the inlet velocity was specified as 10 m/s, and the inlet pressure was calculated by linear extrapolation. In addition, κ and ω were set equal to 10^{-4} and 5.0, respectively, similar to Liu and Zheng (1994). At the outlet, the pressure was set equal to the ambient pressure, and the x and y component velocities as well as κ and ω were calculated from linear extrapolation.

Convergence Criterion

The convergence of the solution was examined by looking at the residual history which is represented by the RMS(ΔU) and the RES(div) values. The RMS(ΔU) value is the Root-Mean-Square of the change of the dependent variables between two consecutive time steps. RES(div) represents the maximum residual of the continuity equation (for all grid points), excluding the unsteady pseudo-pressure term. Figure 5 shows the convergence history for the grid shown in Figure 3.

RESULTS AND DISCUSSION

The calculations for this study were carried out using the pseudo-compressible code described in the proceeding sections on an Alliant FX-2800 supercomputer with eight 40 MHz i860 processors (Each processor is about as fast as a Sparc2 processor). The CPU time needed for one iteration is about 3.702×10^{-4} second per active grid point. The grid that was used is shown in Figure 3 and as stated before, rotation was not included. In addition, a grid with denser grid spacing at the walls (13,677 active vertices) was used which produced similar results. Figures 6, 7, and 8 show the velocity field, velocity magnitude contours, and pressure contours, respectively, for a Reynolds number of 8.5917×10^6 (C = 1.15 for experimental comparison). From these figures, several observations can be noted. First, it can be seen that there is very little flow, in fact some inflow at the outlets, in the two outer branches of the cooling passage. Since there is no rotation, this is likely to be the actual case as there is no driving force on the flow to make a sharp turn around the bottom of the second vertical dividing wall. The pin fins at the entrance to the two upper passages also prevent flow from entering these passages, as they are designed to do when the blade is rotating (Roelke, 1992, and Snyder and Roelke, 1988). Furthermore, it can be seen in Figure 8 that there is no pressure gradient in this region, as most of the pressure drop occurs as the flow goes through the 180 degree turn at the end of the passage divider in the blade tip.

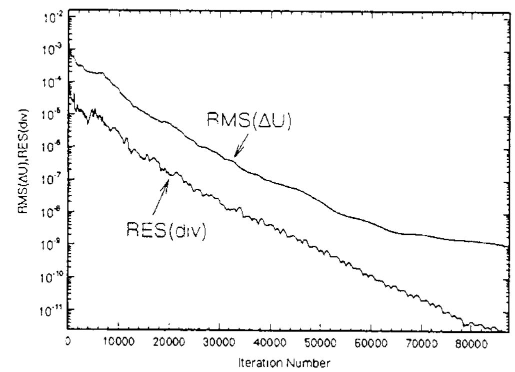

FIGURE 5: CONVERGENCE HISTORY

Also evident in Figure 6 are several regions of recirculation, one in the blade tip, another after the 180 degree turn in the tip which extends all the way down the divider wall, another near the entrance to the cooling passage, and lastly where the second vertical dividing wall meets the outer surface of the blade. Figures 9 and 10 show close-ups of these regions. In particular, Figure 9 shows the beginning of the large recirculation zone after the sharp turn in the blade tip which is also a region of low pressure (Figure 8). This occurs because of the sharp 180 degree turn during which the flow is unable to stay attached to the wall as it goes through an acceleration. Also, because of the comparatively low momentum of the fluid in this study (~10 m/s), the flow is never able to reattach itself to the wall until it hits the bottom surface that is part of the blade hub (Figure 10). These regions of recirculation are explainable, but this may change when rotation is added. In addition, these regions are in essence dead zones where there is no convection present to remove the heat. Depending on the location of these recirculation zones, particularly in the blade tip, this can cause an absence of heat transfer just where it is needed the most. It should be noted, however, that without experimental evidence, these observations cannot be validated.

CONCLUSIONS

In this study, a multi-block structured pseudo-compressible code has been used to simulate the flowfield in the internal cooling passage of a radial turbine blade. The steady, two-dimensional flow was modelled as viscous, turbulent, and non-rotating. A spatially second-order accurate, symmetric TVD scheme was used to solve the hyperbolic system of equations. The turbulence was simulated by using a κ-ω turbulence model.

The preliminary results from this study show the complicated flow field in the turbine blade cooling passage which can give useful insight into the physics of the turbine blade cooling problem. However, comparisons with experimental data must be made to verify these results. In the future, an extension to three-dimensions will be done as well as the introduction of rotation. Finally, the compressible Navier-Stokes equations will be incorporated so that the actual operating conditions of the turbine blade can be modeled.

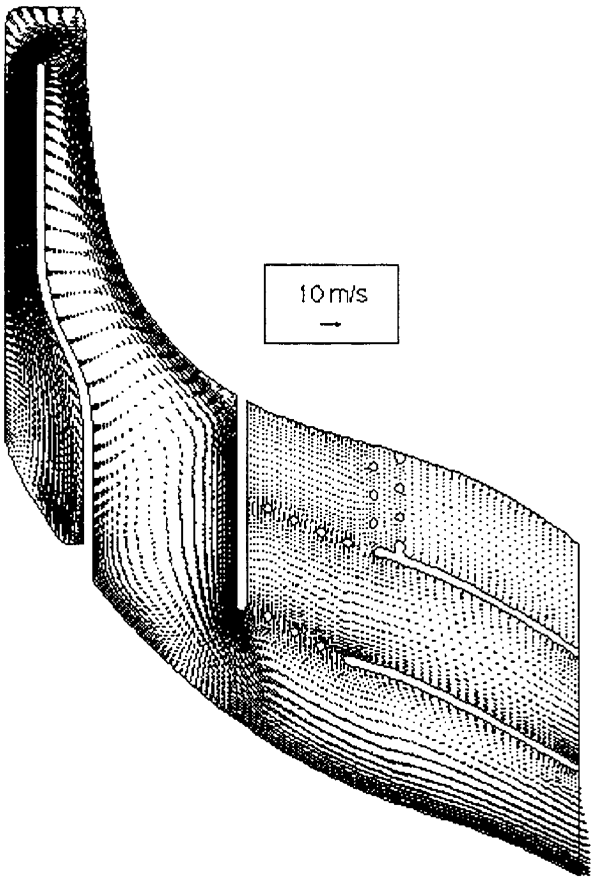

FIGURE 6: VELOCITY VECTOR FIELD

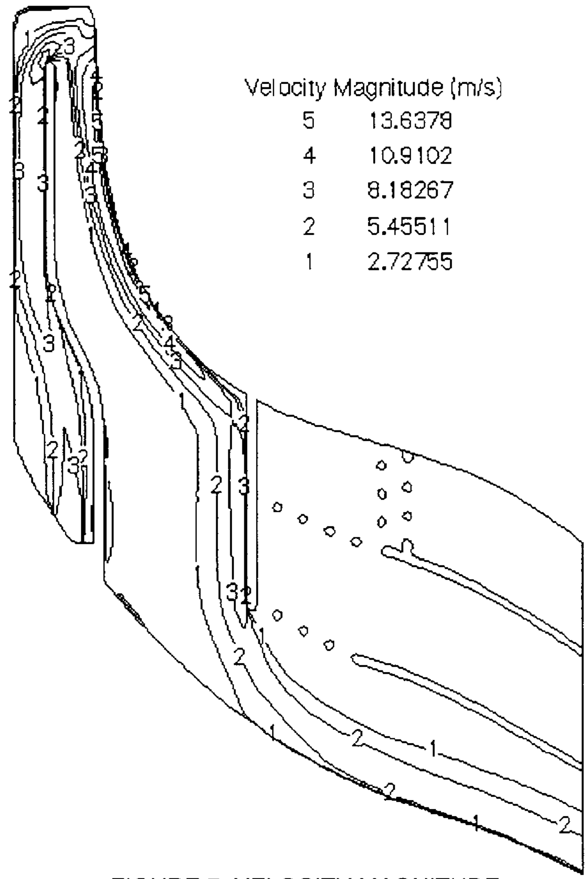

FIGURE 7: VELOCITY MAGNITUDE

ACKNOWLDEGEMENTS

The authors would like to thank the State of Michigan and Michigan Technological University for providing funds for this research through the Research Excellence Fund (MTU # 930938). We would also like to thank Michigan Technological University Advanced Scientific Computer Center for allowing us to use the Alliant FX-2800 computing system.

REFERENCES

Amsden, A.A., 1993, "KIVA-3: A KIVA Program with Block-Structured Mesh for Complex Geometries," LA-12503-MS

Bradbury, L. J. S., Durst, F., Launder, B. E., Schmidt, F. W., and Whitelaw, J. H., 1982, Turbulent Shear Flows 3, Springer-Verlag, Berlin.

Chorin, A. J., 1967, "A Numerical Method for Solving Incompressible Viscous Flow Problems," J. of Comp. Physics, Vol. 2, pp. 12-26.

Cohen, H., Rogers, G.F.C., Sarayanamuttoo, H.I.H., 1987, Gas Turbine Theory, 3rd Edition, John Wiley & Sons Inc., New York.

Haines, A. B., Editor, 1982, "Turbulence Modelling," Aeronautical Journal, August/September, pp. 269-277.

Huang, P. G. and Coakley, T. J., 1992, "An Implicit Navier-Stokes Code for Turbulent Flow Modeling," AIAA Paper No. 92-0547.

Katsanis, T., 1985, "Calculation of Three-Dimensional, Viscous Flow Through Turbomachinery Blade Passage by Parabolic Marching," AIAA/SAE/ASME 21st Joint Propulsion Conference, Paper 85-1405, Monterey, California.

Kumar, G.N., Roelke, R.J., and Meitner, P.L., 1989, "A Generalized One Dimensional Computer Code for Turbomachinery Cooling Passage Flow Computations," NASA TM-102079.

Kwak, D., Chang, J. L., Shanks, S. P., and Chakravarthy, S., 1986, "A Three-Dimensional Incompressible Navier-Stokes Flow Solver Using Primitive Variables," AIAA J., Vol. 24, pp. 390-396.

Lakshminarayana, B., 1986, "Turbulence Modeling for Complex Shear FLows," AIAA J., Vol. 24, No. 12, pp. 1900-1917

Liu, F. and Zheng, X., 1994, "Staggered Finite Volume Scheme for Solving Cascade Flow with a κ-ω Turbulence Model," AIAA J., Vol. 32, No. 8, pp. 1589-1597.

Launder, B. E. and Spalding, D. B., 1974, "The Numerical Computation of Turbulent Flows," Computer Methods in Applied Mechanics and Engineering, Vol. 3, pp. 269-289.

Majumdar, A.K., Pratap, V.S., and Spalding, D.B., 1977, "Numerical Computation of Flow in Rotating Ducts," J. of Fluids

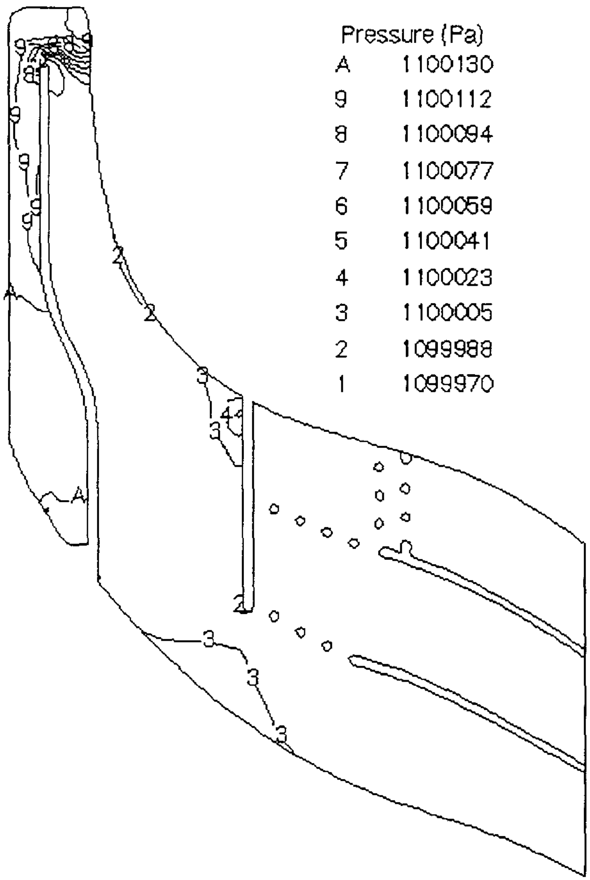

FIGURE 8: PRESSURE CONTOURS

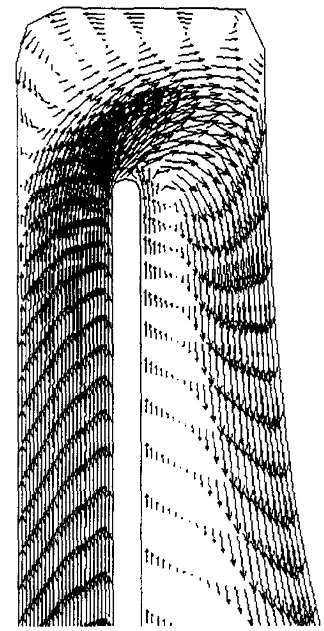

FIGURE 9: MAGNIFIED VIEW OF BLADE TIP REGION

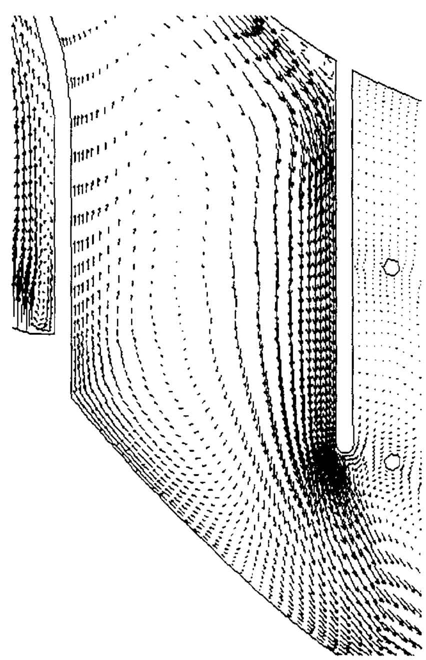

FIGURE 10: MAGNIFIED VIEW OF BLADE HUB REGION

Engineering, Vol.99, pp. 148-153.

Menter, F. R., 1994, "Two Equation Eddy-Viscosity Turbulence Models for Engineering Applications," AIAA J., Vol. 32, No. 8, pp. 1508-1605.

Reynolds, W. C., 1976, "Computation of Turbulent Flows," Annual Review of Fluid Mechanics, Vol. 8, pp. 183-208.

Roelke, R.J., 1992, "Radial Turbine Cooling," NASA TM-105658

Snyder,P.H., and Roelke,R.J., 1988, "The Design of an Air-Cooled Metallic High Temperature Radial Turbine,", AIAA/ ASME/SAE/ASEE 24th Joint Propulsion Conference, Paper AIAA-88-2872, Boston, Massachusetts.

Steger, J.L. and Sorenson, R.L., 1979, "Automatic Mesh-Point Clustering Near a Boundary In Grid Generation with Elliptic Partial Differential Equations," J. of Comp. Physics, Vol.33, pp. 405-410.

Wilcox, D. C., 1988, "Reassessment of the Scale Determining Equation for Advanced Turbulence Models," AIAA J., Vol. 26, No. 11, pp. 1299-1310.

Wilcox, D. C., 1992, "The Remarkable Ability Of Turbulence Model Equations to Describe Transition," 5th Symposium on Numerical and Physical Aspects of Aerodynamic Flows, 13-15 January, California State University, Long Beach, CA.

Wilcox, D. C., 1993a,"Turbulence Modeling for CFD," DCW Industries, Inc., La Cañada, California

Wilcox, D. C., 1993b, "A Two-Equation Turbulent Model for Wall-Bounded and Free-Shear Flows," AIAA Paper 93-2905, Orlando, FL.

Wilcox, D. C., 1994, "Simulation of Transition with a Two-Equation Turbulence Model," AIAA J., Vol. 32, No. 2, pp. 247-255.

Yang, S. L., Chang, Y. L., and Arici, O., 1994a, "Numerical Computation of the NREL Airfoils Using A Symmetric TVD Scheme," 13th ASME Wind Energy Symposium, SED-Vol. 15, pp. 41-49.

Yang, S. L., Chang, Y. L., and Arici, O., 1994b, "Incompressible Navier-Stokes Computation of the NREL Airfoils Using a Symmetric Total Variational Diminishing Scheme," ASME Journal of Solar Energy Engineering (to appear).

Yang, S. L., Chang, Y. L., and Arici, O., 1995a, "Post-Stall Navier-Stokes Computation of the NREL Airfoil Using a κ-ω Turbulence Model," 14th ASME Wind Energy Symposium (to appear).

Yang, S. L., Chang, Y. L., Michalek, D. J., and Arici, O., 1995b, "Investigation of a TVD Scheme for Incompressible Flows Using the Pseudo-Compressible Formulation," First Asian Computational Fluid Dynamics Conference, January 16-19, Hong Kong.

Yee, H.C. and Harten, A., 1987,"Implicit TVD Scheme for Hyperbolic Conservation Laws in Curvilinear Coordinates," AIAA Journal, Vol. 25, pp.266-274.

Yee, H.C., Klopfer, G.H. and Montagne, J.L., 1990,"High-Resolution Shock Capturing Schemes for Inviscid and Viscous Hypersonic Flows," J. of Comp. Physics, Vol. 88, pp.31-61.